Evolution of the Yellow River Delta and its relationship with runoff and sediment load from 1983 to 2011

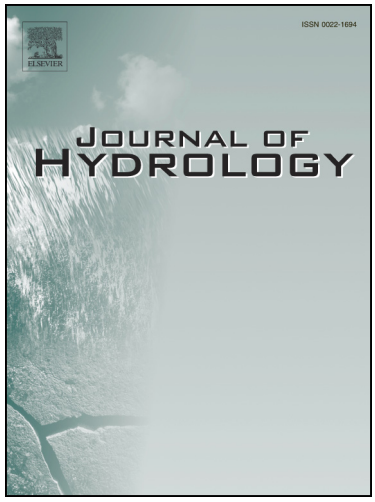

Evolution of the Yellow River Delta and its relationship with runoff and sediment load from 1983 to 2011

Dongxian Kong, Chiyuan Miao, Alistair G.L. Borthwick, Qingyun Duan, Hao Liu, Qiaohong Sun, Aizhong Ye, Zhenhua Di, Wei Gong

PII: S0022-1694(14)00720-3
DOI: http://dx.doi.org/10.1016/j.jhydrol.2014.09.038
Reference: HYDROL 19899

To appear in: *Journal of Hydrology*

Received Date: 22 May 2014
Revised Date: 5 August 2014
Accepted Date: 14 September 2014

Please cite this article as: Kong, D., Miao, C., Borthwick, A.G.L., Duan, Q., Liu, H., Sun, Q., Ye, A., Di, Z., Gong, W., Evolution of the Yellow River Delta and its relationship with runoff and sediment load from 1983 to 2011, *Journal of Hydrology* (2014), doi: http://dx.doi.org/10.1016/j.jhydrol.2014.09.038

Evolution of the Yellow River Delta and its relationship with runoff and sediment load from 1983 to 2011

Dongxian Kong[1], Chiyuan Miao[1,2]*, Alistair G.L. Borthwick[3], Qingyun Duan[1], Hao Liu[4],Qiaohong Sun[1], Aizhong Ye[1], Zhenhua Di[1], Wei Gong[1]

[1]State Key Laboratory of Earth Surface Processes and Resource Ecology, College of Global Change and Earth System Science, Beijing Normal University, Beijing 100875, P.R.China

[2]Yellow River Institute of Hydraulic Research, Key Laboratory of Soil and Water Loss Process and Control on the Loess Plateau of Ministry of Water Resources, Zhengzhou, Henan, 450003

[3]School of Engineering, The University of Edinburgh, The King's Buildings, Edinburgh EH9 3JL, U.K.

[4]Department of Civil and Environmental Engineering, University of California, Irvine, CA 92697, USA

Abstract: Long-term data from a hydrological monitoring station and remotely-sensed satellite images were used to explore the effects of runoff and suspended sediment load on evolution of the Yellow River Delta (YRD) from 1983 to 2011. During this period, an average runoff of 18.0×10^9 m^3 yr^{-1} and an average sediment load of 341×10^6 t yr^{-1} flowed through the delta lobes into the sea. The runoff and sediment load exhibited downward trends with time, along with large inter-annual fluctuations. Three stages were evident in the data. From 1983 to the late 1990s, the Yellow River experienced progressively severe droughts which reduced both runoff and sediment load to its delta lobe. The delta nevertheless grew to a peak area of about 3950 km^2 in 2000. From 2000 to 2003, the YRD area decreased. Meanwhile, the operation of the dam at Xiaolangdi and changes in water consumption driven by a new regulatory framework helped stabilize the runoff. Although the sediment load continued to decline, partly due to sediment check dams along the middle Yellow River and the reduced sediment carrying capacity of the river, the YRD area nevertheless increased between 2003 and 2011. The variations in runoff and sediment load directly influenced changes to

* Corresponding authors. Tel.: +86-10-58804191; fax: +86-10-58804191.

E-mail address: miaocy@vip.sina.com (C. Miao)

the plan-form area, shoreline migration, and morphology of the YRD. From 1983 to 2011, the net land area of the delta increased by 248 km^2, its coastline extended by 36.45 km, and its shape became increasingly irregular due to the emergence of its delta lobes. In 1996, an artificial diversion altered the position of the main delta lobe from Qingshuigou to Qing 8. A stepwise multiple regression analysis indicated that the YRD would have required average sediment loads of about 441×10^6 t yr^{-1} before 1996 and 159×10^6 t yr^{-1} after 1996 to maintain equilibrium.

Keywords： delta; Yellow River; climate change; human activity

1. Introduction

A river delta is formed by the deposition of river sediment as it enters the sea. Deltas simultaneously respond to environmental change by shrinking and expanding over temporal and spatial scales. Both the runoff and sediment load delivered to the sea are dominant factors affecting the evolution of a delta (Yu et al., 2011). Climate change has a direct affect on river delta systems by altering the upstream runoff (Xu, 2005; Wang et al., 2012; Gao et al., 2012). Furthermore, human activities, such as water diversion works, reservoir dam constructions, and soil and water conservation measures (e.g. sediment check dams, contour farming, afforestation, land consolidation, and water pricing) can also radically alter delta ecosystems by influencing the quantities of water and sediment discharging into the sea through the delta lobes (Xu, 2005; Miaoet al., 2010; Wang et al., 2012; Gao et al., 2014a, 2014b). In recent decades, almost all river deltas around the world have been impacted upon by human activities, and the increased frequency and severity of extreme runoff events through climate variability and change. Examples include deltas in the Nile river (El Banna and Frihy, 2009), Ebro River (Mikhailova, 2003), Mississippi River (Snedden et al., 2007), Mekong River (Le et al., 2007), Yangtze River (Yang et al., 2011), Pearl River (Zhang et al., 2010) and Yellow River (Wang et al., 2010). Recent research has established that 85% of the river deltas around the world shrank during the first decade of 21st Century duo to sediment capture in the upstream reaches of their river basins, and it is believed that this situation will become more severe in the future (Syvitski et al., 2009).

The Yellow River Delta (YRD) provides one of the most poignant examples worldwide of the huge impacts on a delta that can arise from increased droughts and human activities affecting water consumption, river regulation, soil conservation, etc. (Miao and Ni, 2009). As the birthplace of ancient Chinese civilization, the lower Yellow River was the most prosperous region in early Chinese history (Yu, 2002) and remains of major socio-economic importance in modern China. The Yellow River is the second largest river in the world in terms of sediment load, with an average of 1.1×10^{9} t yr^{-1} reaching the ocean annually (Milliman and Meade, 1983). Approximately 30 – 40 % of the sediment transported to the sea is deposited at the delta lobe at the mouth of the Yellow River, forming the YRD (Li et al., 1998). Over the past 30 years, many research studies have been carried out on the YRD due to its socio-economic importance and unique ecological environment (Cui et al., 2009). For example, the YRD contains the second largest oilfield in China (Shengli Oilfield). It is also rich in biological resources and is home to 1,543 wild animal species, 393 seed plant species,

and 283 bird species (including 9 species qualifying as first-level nationally protected birds, and 42 at the second level) (Zhang et al., 1998). The YRD wetland is an important habitat and transfer area for many rare and endangered migrating birds, such as the red-crowned crane, hooded crane, Siberian crane, oriental stork, black stork, and golden eagle (Xu et al., 2002). In recent decades, the combination of decreasing runoff and sediment load due to increasing occurrences and severity of low-flow events (Yang et al., 1998) exacerbated by the influence of human activities (Fan et al., 2006a) have led to significant modifications to the YRD, including changes to its wetland landscape, biodiversity and deltaic configuration (Cui et al., 2013; Higgins et al., 2013).

Previous studies primarily focused on the qualitative relationship between the evolution of YRD and the stream-flow and sediment load in the delta lobe (Chu et al., 2006; Peng et al., 2010; Wang et al., 2010; Yu et al., 2011), land-use of the YRD (Chen et al., 2011; Zhang et al., 2011; Miao et al., 2012b; Ottinger et al., 2013), and shoreline changes (Cui and Li, 2011; Yang, 2012; Liu et al., 2013). Less attention was paid to quantitative contribution of runoff and sediment load on the YRD, the influence of artificial shifts of the course of the main delta lobe channel on the overall balance of the YRD, and the impacts of drought and human activities in the Yellow River basin on the evolution of YRD.

The aim of the present study is to examine the evolution of the Yellow River delta from 1983 to 2011 during which major droughts occurred (due to a combination of reduced runoff caused by climate change, increased water consumption driven by population change, rapid socio-economic development and poor irrigation practice), an artificial diversion of the delta lobe was implemented, a major reservoir began operation for flushing sediment and flood control, and changes that took place in regulation practice by the Yellow River Conservancy Commission from water and soil conservancy to an integrated framework. The YRD therefore provides a very useful exemplar to scientists, engineers, environmentalists and decision makers as a case study of the effects of drought-driven and anthropogenic changes to a key river delta. This paper analyzes the variations in runoff and sediment load in the Yellow River, and their effect on the morphological evolution of the delta. An assessment is made of the threshold values of sediment load required to main the equilibrium of the delta before and after artificial diversion led to a new delta lobe at Qing 8 in 1996. An error analysis is included. The insights gained about the temporal behavior of the YRD should be useful to decision makers weighing up future options for large-scale constructions and environmental protection measures affecting the YRD.

2. Yellow River Delta: study area, event chronology, and data sources

2.1. Study area

The YRD is located in the northeast of Shandong Province, China (Figure 1). The northern and eastern portions of the YRD are adjacent to the Bohai Sea and Laizhou Bay. Three large artificial diversions of the main channel in the YRD were implemented in the past five decades (Fan et al., 2006b; Syvitski and Saito, 2007). In July 1964, the course of the Yellow River delta lobe was altered artificially from the Shenxiangou route to the Diaokou course to help alleviate potential flood problems. In May 1976, development of the Shengli Oilfield caused the delta lobe to shift course into the Bohai Sea through the Qingshuigou River. In August 1996, the main channel of the delta lobe was diverted northeast to the 8th section of the Qingshuigou River forming the Qing 8 course (Xu et al., 2002) in order to facilitate the offshore to onshore operation of the Xintan and Kendong Oilfields. Since then, the course of the delta lobe of the Yellow River has remained essentially unchanged, apart from some minor movements.

Figure 1

The YRD region is characterized by a warm-temperate continental monsoon climate with distinct seasons (Sun et al., 2014). The annual mean temperature ranges from 11.5 to 12.4 ^{o}C, with highest monthly temperature of 26.6 ^{o}C in July and lowest of -4.1 ^{o}C in January. The YRD is located in a semi-arid zone where the annual rainfall is 590.9 mm and pan evaporation exceeds 1500 mm. The monthly maximum rainfall is 227 mm in July and the minimum rainfall is 1.7 mm in January. Approximately 70% of the total annual precipitation occurs in the summer. Dominant soil types are alluvial and saline (Fang et al., 2005). Sediment in the Yellow River discharging into the sea has a composition of between 8-28 % sand, 64-78 % silt, and 6-21 % mud (Lim et al. 2006). Sediment transport is primarily as suspended sediment. There is almost no bed load in the Yellow River. The median grain size of the suspended sediment is 0.015-0.025 mm at Lijin station (Xu, 2000). Natural vegetation in the YRD primarily comprises Phragmites australis, Suaeda heteroptera, Tamarix chinensis, Triarrhena sacchariflora, Myriophyllum spicatum, and Limonium sinense (Jiang et al., 2013).

2.2. Chronology of hydrological and human impacts on the Yellow River from 1983-2011

The lower Yellow River experienced substantial hydrological and human impacts during the study period. From the 1970s to the late 1990s, the river suffered increasingly severe droughts, during which progressively increasing numbers of no-flow and nearly no-flow events occurred close to the delta mouth. El Niño/Southern Oscillation (ENSO) events affected the strength of monsoons passing over the Tibetan plateau where the source catchment is located. The drought events were caused by a combination of factors including climate change leading to increased temperature and decreased precipitation in the upper catchment areas, poor irrigation practice along the middle reaches, and increased water consumption linked to enhanced socio-economic development and some population growth. Man-made constructions also had a major effect on the lower Yellow river and YRD, in particular the artificial diversion of the delta lobe in 1996 and the construction from 1994 to 2000 and operation from about 2000 of the reservoir-dam at Xiaolangdi. By 2000, the condition of the lower Yellow River was a major national concern in China, considerable investment was made into remediation of the lower Yellow River, and the Yellow River Conservancy Commission altered its approach from a conservancy framework related to flood control (e.g. Yellow River Water Allocation Plan in 1987) to an integrated one of sustainability involving water saving and water pricing policies (Li, 2003). Since 2000, the Yellow River has flowed continuously to the sea, but there remain major concerns about its vitality.

2.3. Data sources

The study utilized multi-temporal remotely-sensed Landsat data from a Multispectral Scanner (MSS), a Thematic Mapper (TM) and an Enhanced Thematic Mapper (ETM+) obtained in the period from 1983 to 2011, totaling 29 scenes (Table 1) archived by the Earth Resources Observation and Science (EROS) Center (http://glovis.usgs.gov/). All data accounted for the impact of cloud cover. The spatial resolution of the MSS, TM and ETM+ data were 80 m, 30 m and 30 m (Tucker et al., 2004; Chander et al., 2009). According to the Worldwide Reference System, one full MSS (path 130, row 34) or TM (path 121, row 34) scene fully covered the study area. Data on annual runoff and suspended sediment load at selected hydrological stations from 1983 to 2011 were obtained from the Yellow River Conservancy Commission (YRCC). The annual regional precipitation series were interpolated from data from 175 meteorological stations, which were

provided by the National Meteorological Information Center of the China Meteorological Administration.

Table 1

3. Methodology

In practice, coastline extraction methods include manual photointerpretation techniques by experts, and computational methods such as edge-detection (Lee and Jurkevich, 1990; Mason and Davenport, 1996), neural networks (Ryan et al., 1991), locally adaptive thresholding (Liu and Jezek, 2004), fuzzy connectivity (Dellepiane et al., 2004), mathematical morphology (Geleynse et al., 2012) and pulse coupled neural networks (Del Frate et al., 2012). The present study applied an interactive interpretation technique combining an automatic boundary detection algorithm with human supervision to detect the land-ocean shoreline boundaries in satellite images. The automatic boundary detection procedure consisted of four steps. First, we calculated the background trend to remove specular reflection of solar radiation on non-flat water surfaces. Second, we applied a noise-removing algorithm to reduce scattered noise contaminating the satellite images. Third, we chose adaptively a threshold that differentiated the land from the ocean, and then transformed the data into black-white (BW) binary form. Finally, we employed an automatic boundary-detection algorithm to locate boundaries in the BW-images, and verified or adjusted them with reference to a combined TM 432 pseudo-color image. MatLab(R) and its Image Processing Toolbox were used to implement the algorithm and batch-process all the Landsat imageries.

Provided the distributary channels are free to migrate across a delta plain, then widespread sedimentation occurs (Syvitski et al., 2009). This means that a river delta tends to be part of circle, if without artificial control. It is well-established that the YRD is a typical fan-shaped delta (Sun et al., 2002; Chu et al., 2006). The radius of the circle can be calculated from either its area as R_S or its perimeter as R_L. Variations in R_S and R_L represent changes to the river delta. An increase in R_S indicates accretion of the delta area, whereas a decrease indicates erosion. An increase in R_L indicates extension of the coastline, whereas a decrease indicates shortening. The delta radius ratio, R_S / R_L, can be used to characterize the morphology of the YRD. A value close to 1 indicates the shoreline follows a nearly smooth arc, and thus the delta is developing in a spatially uniform manner. A value well away from 1 indicates a tortuous shoreline and that the delta is developing an

irregular shape. Values for R_S, R_L and the radius ratio are determined using the following formulas:

$$R_S = 2\sqrt{\frac{S}{\pi}} \quad (1)$$

$$R_L = \frac{2L}{\pi} \quad (2)$$

$$C = \frac{R_S}{R_L} = \frac{\sqrt{\pi S}}{L} \quad , \quad (3)$$

where S is the area of the YRD, L is the length of the coastline, and C is the delta radius ratio.

4. Results and discussion

4.1. Runoff and sediment load in the Yellow River

Lijin hydrological station is located approximately 100 km upstream from the river mouth (Figure 1a), and is the final hydrological gauging station in the Yellow River used for monitoring the water-sediment delivery process into the Bohai Sea. In accordance with previous research (Wang et al., 2010), we used the runoff and sediment load measured at Lijin hydrological station to represent the delivery characteristics in the Yellow River delta lobe, noting that about 1.7 % of the Yellow River sediment load passing Lijin is deposited in the river course before reaching the sea (Hu and Cao, 2003). Figure 2 shows the temporal behavior of annual runoff and sediment load at Lijin hydrological station from 1983 to 2011. During this period, the average annual runoff is 18.0 $\times 10^9$ m^3 and average annual sediment load is 341$\times 10^6$ t. The maximum annual values for runoff of 49.08$\times 10^9$ m^3 and sediment load of 1024$\times 10^6$ t occurred in 1983, and the minimum annual values of runoff of 1.86$\times 10^9$ m^3 and sediment load of 16$\times 10^6$ t occurred in 1997. There is a positive linear correlation between the runoff and sediment load, with a correlation coefficient of 0.61, which is 99 % significant. From the variations evident in the plot, the 29-year (1983-2011) series of runoff and sediment load can be divided into three stages, i.e., before 2000, 2000-2002 and after 2002.

Figure 2

Before 2000, the runoff and sediment load in the Yellow River exhibited downward trends, with mean runoff of 20.2$\times 10^9$ m^3 yr^{-1} and mean sediment load of 488$\times 10^6$ t yr^{-1}, well below the

220 average values for the 1970s (31.1×10^9 m^3 yr^{-1} and 898×10^6 t yr^{-1} respectively). From the 1980s
221 onwards, the strength of monsoons in China weakened substantially, leading to significant droughts
222 in North China, and particularly affecting much of Yellow River Basin (which is located in arid and
223 semi-arid regions). From 1983 to 2000, annual precipitation in the Yellow River Basin declined
224 overall whilst annual temperature increased, the latter due to global warming (Figure 3). The higher
225 temperatures significantly accelerated evaporation, resulting in further decrease in runoff (Figure
226 2a). The large fluctuations in precipitation in the Yellow River Basin were possibly linked with El
227 Niño/Southern Oscillation (ENSO) events (Wang et al., 2006a). Human activities also had a
228 significant effect on runoff and sediment loads into the sea (Miao et al., 2011). The population
229 along the Yellow River Basin swelled, causing significant increases in domestic, agricultural and
230 industrial water consumption (Peng et al., 2010). Water was wasted through poor irrigation and
231 relatively unregulated land-use practices. A direct consequence of the reduced precipitation and
232 increased water abstraction was the drying up of the Yellow River, experienced as no-flow events
233 (Figure 4). Hydrological records from Lijin hydrological station show that the total of seasonal
234 no-flow events along the Yellow River channel reached 940 days after 1982, including 901 days in
235 the 1990s. The most serious series of droughts in the Yellow River occurred in 1997, when no-flow
236 events occupied a total of 226 days (Figure 4), resulting from far below normal rainfall and runoff
237 in the Yellow River basin (Figure 2).
238
239 **Figure 3**
240 **Figure 4**
241
242 No further no-flow events have been recorded along the Yellow River from 2000 to date. In
243 the period from 2000-2002, the amounts of runoff and sediment load entering the sea remained at
244 low levels. The mean runoff of 4.57×10^9 m^3 yr^{-1} and mean sediment load of 32×10^6 t yr^{-1}
245 corresponded to 77 % and 93 % reductions compared to their counterpart values in the period from
246 1983-2000. In addition to the decline in precipitation, the construction and operation of large
247 reservoirs played a significant role during the second stage from 2000 to 2002. By 2001, more
248 than 3,147 reservoirs had been built in the Yellow River Basin, with a total storage capacity of 57.4
249 $\times10^9$ m^3 (Zhang et al., 2001). Of these, the Xiaolangdi Reservoir had the greatest effect (Zhang et
250 al., 2011). The Xiaolangdi Reservoir (Figure 1a) became operational during 1999-2001, with a total

storage capacity of 12.7×10^9 m^3. During this period, Xiaolangdi's primary operating mode involved water storage and sediment retention (Figure 5b), greatly reducing the runoff and sediment load reaching the YRD. Since 2002, the Yellow River Conservancy Commission (YRCC) has performed more than 10 flushing operations to regulate the flow of water and sediment into the lower reaches of the Yellow River through the coordinated operation of Xiaolangdi and other reservoirs (Table 2). The regulation primarily involved release of water stored upstream of the Xiaolangdi dam to scour sediment that had been accreting on the bed of the downstream channel, and hence control the flood risk posed by the resulting 'hanging river'. These regulation measures had a direct impact on hydrological processes in the drainage area of the lower Xiaolangdi catchment, and also influenced the river flux delivery to the Bohai Sea .

Table 2

Figure 5

After 2003, the runoff and sediment load maintained higher values than in the second stage, with a mean annual runoff of 18.33×10^9 m^3 yr^{-1} and a mean annual sediment load of 167×10^6 t yr^{-1}. Relative to the first stage, the runoff essentially returned to the same level to that of the mid-1990s, whereas the sediment load remained at low values, steadily decreasing with time. This behavior is primarily due to the water and sediment regulation activities at Xiaolangdi, along with the soil and water conservation efforts along the middle reaches of the Yellow River.

At Sanmenxia hydrological station, both the annual runoff and sediment load decreased significantly with time (Figure 5), indicating the effectiveness of the soil and water conservation and ecological restoration practices implemented on the Loess Plateau. The variations in runoff about the trend may be attributed to variations in the monsoon climate during the wet season promoted by El Niño/Southern Oscillation (ENSO) events. Compared to Sanmenxia station, Huayuankou experienced a lower sediment load and a higher level of runoff over time (Figure 5). From 1983-1999, the annual average runoff increased by 9% and annual average sediment load reduced by 13% at Huayuankou relative to Sanmenxia. From 2003-2011, the annual average runoff at Huayuankou increased by 17% and the annual average sediment load reduced by 67% compared with Sanmenxia. These results demonstrate that the construction and operation of the Xiaolangdi Reservoir played a significant role in water and sediment regulation of the lower Yellow River

(Table 2). Although each water and sediment regulation activity typically lasted about one month, the effect on sediment transport was huge. By 2011, the water and sediment discharges due to regulation activities accounted for 27% and 42% of the total discharges, indicating that the sediment transport capacity had been significantly improved. The foregoing analysis highlights the increasingly prominent impact of human activities on runoff and sediment loads.

4.2 The Evolution of the Yellow River Delta from 1983 to 2011

4.2.1 Area changes

Figure 6 shows the annual values of plan-form area of the YRD as a function of year from 1983 to 2011. It can be discerned that the YRD increased in area by about 248 km^2 during the study period. The changing area exhibits three trends; a steady increase from 1983 to 2000 when the area reached a peak value of 3,924 km^2; a rapid decrease at a rate of 68 km^2 yr^{-1} from 2000 to 2003, and then a more gradual increase from 2003 onwards (Figure 6). We therefore divide the area changes into a rapid growth stage (1983-2000), a retreat stage (2000-2003), and a recovery stage (2003-2011), all in response to the variations in runoff and sediment load. The rapid growth stage was dominated by the twin effects of drought and excess water consumption. The retreat stage coincided with the reservoir at Xiaolangdi initially becoming operational, and the implementation of water conservation measures and improved irrigation and land-use. The recovery stage indicates that the measures may not have been sufficient to prevent further growth of the delta, and may be linked to the development of the new delta lobe at Qing 8 that was initially created in 1996.

Figure 6

Figure 7 presents satellite images in selected years, highlighting the changing shape of the Yellow River Delta with time. Figure 8 shows the migration of the Yellow River Delta coastline from 1983 to 2011. From 1983 to 1996, the delta lobe of the YRD evolved forward at a mean rate of 20.97 km^2 yr^{-1} as an extension of the Qingshuigou channel (Figure 7A-G). From Figure 8A it can be deduced that the growing delta lobe progressed forward at an average rate of 1.4 km yr^{-1}. By 1996, an obvious promontory had formed (Figure 7G). After 1996, the shoreline and area started to extend forward as a new delta lobe in the northeast direction along the Qing 8 channel. Meanwhile

the old Qingshuigou promontory began to retreat because of net erosion once the water and sediment supply became cut off (Figure 7H-O and Figure 8A). From 1997 to 2000, the YRD continued to evolve, with simultaneous extension of the Qing 8 delta lobe and erosion of the Qingshuigou promontory. Apart from sediment load, several other factors influence the short-term evolution of a delta, including sediment grain size (Edmonds and Slingerland, 2007), sediment cohesion (Edmonds and Slingerland, 2010), sediment feed point (Kim et al., 2009) and river plume behavior (Falcini et al., 2012). Given that there was no significant change of river plume behavior and sediment characteristics, the drastic change in land area of the YRD in the late 1990s and early 2000s was most likely due to the relatively low runoff and sediment load (Figure 2) (Liu et al., 2012a). Meanwhile, coastal erosion remained basically unchanged. Both the Qingshuigou and the Qing 8 delta lobes eroded gradually during 2000 to 2003 (Figure 8B). With the restoration of runoff and sediment load (Figure 2), the area of the YRD began to increase incrementally after 2003 (Cui and Li, 2011), the trend having a mean rate of 17.1 km^2 yr^{-1} . Figure 8C shows the growth of the Qing 8 lobe while the old Qingshuigou lobe retreated during 2003 to 2011. Although the total plan-form area of the YRD increased by 3.7% from 2003 to 2011, the area declined by 1.7% from 2000 to 2011. Fixing the annual runoff and sediment load at their 2011 values, more than a decade would be required for the YRD to recover to the area it had in 2000.

Figure 7

Figure 8

4.2.2 Coastline migration

Over time, the length of coastline of the YRD increased, unlike its area (Figure 9), indicating that the coastline was becoming more and more tortuous. From 1983 to 2011, the length of the coastline increased by 36.45 km, equivalent to an average annual growth of 1.3 km. Both coastline extension and retreat occurred during this period, with a coefficient of variation of about 7.8 %, which is higher than the corresponding value for the land area. Comparison between the annual changes in YRD area and YRD coastline indicated that the changes were not correlated. For example, as the delta shrank, its area reduced but its shape became increasingly contorted thus increasing the length of its coastline.

Figure 9

4.2.3 Morphological changes

Figure 10 shows the variation with time of the delta radius ratio, R_S / R_L, which provides a measure of the evolution of the shape of the entire YRD from 1983 to 2011. Despite the considerable inter-annual fluctuations evident, the delta radius ratio exhibits a decreasing trend over time, indicating that the morphology of the YRD became increasingly irregular over the study period. Taking spot values at either end of the period, the delta radius ratio of the YRD fell from 0.68 in 1983 to 0.57 in 2011. The delta radius ratio had a coefficient of variation of 7.8 %, which is very similar to that obtained for the coastline length. This is hardly surprising, given the close linkage between the morphology of the YRD and the shifts occurring to its river course and the associated dynamic changes in orientation of the delta lobe. It is well known that many factors influence the orientation of delta lobes, including near-shore currents (Li et al., 2001), Coriolis force (Fan et al., 2006a), water-sediment processes (Wang et al., 2005) and local terrain conditions. In 1983, the Qingshuigou channel mouth experienced major siltation, with the emergence of many small branch channels and sand bars separating the channels (Figure 11A). In 1984, the direction of the Qingshuigou channel mouth altered from east to southeast, and a promontory formed over the next 12 years (Figure 11B). Meanwhile, the delta radius ratio decreased from 0.68 to 0.62. After a further artificial channel diversion in 1996, a new delta lobe began rapidly to develop from the Qing 8 channel (Figure 11C). From 1996 to 2007, the YRD became more irregular, with its delta radius ratio declining from 0.62 to 0.54. Due to heavy erosion related to bank bursts, multiple branches appeared along the north side of the river mouth (Figure 11D). Excessive runoff during the flood season of 2007 caused the Qing 8 channel mouth to divert northward by 2 km. After 2007, the orientation of the Yellow River mouth continued further northward. By 2011, the direction of the river mouth was almost directly north, and the tip of the delta lobe was no longer sharp (Figure 11E). This change led to a more spatially uniform development of the delta, with its radius ratio increasing from 0.54 in 2007 to 0.57 in 2011.

Figure 10

Figure 11

4.3 Relationship between evolution of YRD and variations in runoff and sediment load

Evolution of the YRD is influenced by several key factors (see e.g. Chu et al., 2006), including river discharge, sediment input, wave energy, tidal regime, littoral currents etc. Changes to any of these factors could affect the geomorphological and sedimentological regimes of the delta (Wang et al., 2010). In particular, interactions among soil, fluvial and coastal dynamics are responsible for enhancing the relative roles between sedimentation and erosion at delta lobes, thus controlling the growth and shape of the overall delta. For the YRD to be in equilibrium and its area remain constant, the rate of river sediment accumulation must equal the erosion rate due to near-shore coastal flows. When the accumulation rate of river sediment is less than the coastal erosion rate, the YRD starts to shrink and its area consequently reduces. Conversely, when the accumulation rate of river sediment is higher than the coastal erosion rate, the delta lobe extends further and the area of the YRD increases. Over the past 30 years, the near-shore coastal dynamics has hardly varied at the Yellow River mouth (Wang et al., 2010; Hu and Cao, 2003) and so changes to the river flux appear to be the key factor controlling the evolution of the delta (Fan et al., 2006b). A previous study has shown that the threshold value of river flux required to keep the YRD stable varies for different channels (Wang et al., 2006b). Obviously, the riverbed features and coastal dynamics are particular to each channel, affecting the depositional characteristics of sediment delivered into the sea.

Noting that the runoff and sediment reached the sea through different channels before and after the artificial diversion of the main delta lobe from Qingshuigou to Qing 8 was introduced in 1996, we carried out stepwise multiple regression analysis over two phases, 1983-1995 and 1997-2011. The regression analysis indicated that river sediment load is a dominant factor influencing the evolution of the YRD. However, taking runoff and sediment load simultaneously into account, the results from the regression analysis indicated no further contribution from runoff, which is reasonable given the significant correlation between the annual sediment load and annual runoff. Here, we define the annual area change in the i+1 th year as the arithmetic difference between the area of the YRD in the i+1 th year minus that in the i th year. The linear regression functions obtained between the annual sediment load (x, 10^9 t) and the annual change in area of YRD (y, km^2) for the two phases before and after 1996 are:

$$y = 0.1758x - 77.466 \quad R^2 = 0.3 \quad P = 0.0 \quad \text{before 1996} \quad (4)$$

$$y = 0.3317x - 52.8 \quad R^2 = 0.4 \quad P = 0.0 \quad \text{after 1996} \quad (5)$$

Figure 12 plots the YRD area change against sediment load along with the regression lines, for both phases. Although scatter is evident, the trends are of increasing area changes with sediment load. Using equations (4) and (5), the annual change in area of YRD is zero and equilibrium is achieved when the average annual sediment load equals 441×10^6 t in 1983-1995 and 159×10^6 t in 1997-2011. These threshold values of sediment load are substantially different, demonstrating again the important influence of the river flux characteristics on the evolution of the delta.

Figure 12

4.4 Error analysis

The exact position of the coastline of YRD varies with time and tide, and so errors are introduced to the analysis when comparing coastlines extracted from satellite images acquired at different times in any given day. Although researchers initially held the view that the tidal effect is weak and can be ignored for the Yellow River estuary (Chu et al., 2006), more recently Liu et al. (2012b) reported that tidal and landform variations can have a significant influence on the detection of coastline changes in the Yellow River delta. Liu et al. evaluated the maximum error caused by the tidal effects, assuming that the entire coastline remains parallel under different tidal conditions, and regarding the error in delta area as the product of the maximum coastline distance and coastline length. Liu et al. then found the maximum distance among the coastlines for YRD in the same day is less than 172 m. In the present study, the extracted total coastline length and delta area are less than 210 km (Figure 9) and 3950 km^2 (Figure 6), and so, using the foregoing method, the maximum relative error is about 1.1 % of the total delta area. Table 3 lists the relative error in the annual extracted delta area.

5. Conclusions

Previous studies have identified climate change and local human activities as two primary factors that impact on the evolution of river deltas. This paper has focused on recent changes taking place to the Yellow River delta. We found that the runoff and sediment load at the mouth of the Yellow

River exhibited downward trends with great inter-annual variations during the period from 1983 to 2011. These temporal variations in runoff and sediment load directly affected the evolution of the YRD, including its area change, shoreline migration and morphology. The downward trends in runoff were linked to progressively reduced precipitation due to climate warming, and increasing water consumption connected with poor irrigation practice and rapid socio-economic development. The trends in sediment load are largely due to soil conservation measures including 100,000 check dams along the main river and the reduced sediment carrying capacity of the river due to the reduced runoff. The inter-annual fluctuations have been previously related to El Niño/Southern Oscillation (ENSO) events affecting monsoon rainfall in the upper Yellow River catchment. Over the time period considered, the area of the YRD underwent three stages of evolution: a rapid growth stage (1983-2000), a retreat stage (2000-2003) and a recovery stage (2003-2011). Operation of the Xiaolangdi reservoir and implementation of new water consumption policies by the Yellow River Conservancy Commission helped drive changes to the delta area during the retreat and recovery stages. From 1983 to 2011, the delta area increased by 248 km^2 and its coastline grew by 36.45 km in length. During this period, the shape of the entire YRD became more and more irregular because of the emergence of the Qingshuigou and the Qing 8 delta lobes. Multi-step regression analysis indicated that average river sediment loads of ~ 441×10^6 t yr^{-1} and 159×10^6 t yr^{-1} would have been necessary to maintain equilibrium of the YRD area in the periods where the main delta lobe followed the Qingshuigou route in 1983-1996 and the Qing 8 route in 1996-2011.

Acknowledgments

Funding for this research was provided by the Open Foundation of Key Laboratory of Soil and Water Loss Process and Control on the Loess Plateau of Ministry of Water Resources (2014005), the National Natural Science Foundation of China (no. 41001153), Beijing Higher Education Young Elite Teacher Project and State Key Laboratory of Earth Surface Processes and Resource Ecology.

References

Chander, G., Markham, B.L., Helder, D.L., 2009. Summary of current radiometric calibration coefficients for Landsat MSS, TM, ETM+, and EO-1 ALI sensors. Remote sensing of environment, 113(5): 893-903.

Chen, J., Wang, S., Mao, Z., 2011. Monitoring wetland changes in Yellow River Delta by remote

sensing during1976-2008. Progress in Geography, 30(05): 585-592.

Chu, Z.X., Sun, X.G., Zhai, S.K., Xu, K.H., 2006. Changing pattern of accretion/erosion of the modern Yellow River (Huanghe) subaerial delta, China: Based on remote sensing images. Marine Geology, 227(1-2): 13-30.

Cui, B., Li, X., 2011. Coastline change of the Yellow River estuary and its response to the sediment and runoff (1976–2005). Geomorphology, 127(1-2): 32-40.

Cui, B., Yang, Q., Yang, Z., Zhang, K., 2009. Evaluating the ecological performance of wetland restoration in the Yellow River Delta, China. Ecological Engineering, 35(7): 1090-1103.

Cui, G., Zhang, X., Zhang, Z., Xu, Z., 2013. Changes of coastal wetland ecosystems in the Yellow River Delta and protection countermeasures to them. Asian Agricultural Research, 5(1): 48-50.

Del Frate, F., Latini, D., Minchella, A., Palazzo, F., 2012. A new automatic technique for coastline extraction from SAR images, SPIE Remote Sensing. International Society for Optics and Photonics, 8536:85360R.

Dellepiane, S., De Laurentiis, R., Giordano, F., 2004. Coastline extraction from SAR images and a method for the evaluation of the coastline precision. Pattern Recognition Letters, 25(13): 1461-1470.

Edmonds, D.A., Slingerland, R.L., 2007. Mechanics of river mouth bar formation: Implications for the morphodynamics of delta distributary networks. Journal of Geophysical Research, 112: F02034.

Edmonds, D.A., Slingerland, R.L., 2010. Significant effect of sediment cohesion on delta morphology. Nature Geoscience, 3(2): 105-109.

El Banna, M.M., Frihy, O.E., 2009. Human-induced changes in the geomorphology of the northeastern coast of the Nile delta, Egypt. Geomorphology, 107(1-2): 72-78.

Falcini, F. et al., 2012. Linking the historic 2011 Mississippi River flood to coastal wetland sedimentation. Nature Geoscience, 5(11): 803-807.

Fan, H., Huang, H., Zeng, T., 2006a. Impacts of anthropogenic activity on the recent evolution of the Huanghe (Yellow) River Delta. Journal of coastal research, 22(4): 919-929.

Fan, H., Huang, H., Zeng, T.Q., Wang, K., 2006b. River mouth bar formation, riverbed aggradation and channel migration in the modern Huanghe (Yellow) River delta, China. Geomorphology, 74: 124-136.

496 Fang, H., Liu, G., Kearney, M., 2005. Georelational analysis of soil type, soil salt content, landform,
497 and land use in the Yellow River Delta, China. Environmental management, 35(1): 72-83.
498 Gao, Y., Zhu, B., Wang, T., Wang, Y.F., 2012. Seasonal change of non-point source
499 pollution-induced bioavailable phosphorus loss: a case study of Southwestern China.
500 Journal of Hydrology, 420-421: 373-379
501 Gao, Y,, et al., 2014a. Phosphorus and carbon competitive sorption-desorption and associated
502 non-point loss respond to natural rainfall events. Journal of Hydrology, 517:447-457.
503 Gao, Y., et al., 2014b. Water use efficiency threshold for terrestrial ecosystem carbon sequestration
504 under afforestation in China. Agricultural and Forest Meteorology, 195-196, 32-37.
505 Geleynse, N., Voller, V.R., Paola, C., Ganti, V., 2012. Characterization of river delta shorelines.
506 Geophysical Research Letters, 39(17): L17402.
507 Higgins, S., Overeem, I., Tanaka, A., Syvitski, J.P.M., 2013. Land subsidence at aquaculture
508 facilities in the Yellow River delta, China. Geophysical Research Letters, 40(15):
509 3898-3902.
510 Hu, C., Cao, W., 2003. Variation, regulation and control of flow and sediment in the Yellow River
511 Estuary: I. Mechanism of flow-sediment transport and evolution. Journal of Sediment
512 Research, 5: 1-8.
513 Jiang, D., Fu, X., Wang, K., 2013. Vegetation dynamics and their response to freshwater inflow and
514 climate variables in the Yellow River Delta, China. Quaternary International, 304: 75-84.
515 Kim, W., Dai, A., Muto, T., Parker, G., 2009. Delta progradation driven by an advancing sediment
516 source: Coupled theory and experiment describing the evolution of elongated deltas. Water
517 Resources Research, 45(6): W06428.
518 Le, T.V.H., Nguyen, H.N., Wolanski, E., Tran, T.C., Haruyama, S., 2007. The combined impact on
519 the flooding in Vietnam's Mekong River delta of local man-made structures, sea level rise,
520 and dams upstream in the river catchment. Estuarine, Coastal and Shelf Science, 71(1-2):
521 110-116.
522 Lee, J. S., Jurkevich, I., 1990. Coastline detection and tracing in SAR images. Geoscience and
523 Remote Sensing, IEEE Transactions on, 28(4): 662-668.
524 Li, G., Tang, Z., Yue, S., Zhuang, K., Wei, H., 2001. Sedimentation in the shear front off the Yellow
525 River mouth. Continental Shelf Research, 21(6–7): 607-625.
526 Li, G., Wei, H., Han, Y., Chen, Y., 1998. Sedimentation in the Yellow River delta, part I: flow and

527 suspended sediment structure in the upper distributary and the estuary. Marine Geology,
528 149(1): 93-111.
529 Li, G. 2003 Ponderation and Practice of the Yellow River Control, Yellow River Conservancy
530 Press.
531 Lim D.I., Jung H.S., Choi J.Y., Yang S., and Ahn K.S., 2006. Geochemical compositions of river
532 and shelf sediments in the Yellow Sea: Grain-size normalization and sediment provenance.
533 Continental Shelf Research, 26: 15-24
534 Liu, F., Chen, S., Peng, J., Chen, G., 2012a. Temporal variations of water discharge and sediment
535 load of Huanghe River, China. Chinese Geographical Science, 22(5): 507-521.
536 Liu, H., Jezek, K.C., 2004. Automated extraction of coastline from satellite imagery by integrating
537 Canny edge detection and locally adaptive thresholding methods. International Journal of
538 Remote Sensing, 25(5): 937-958.
539 Liu, Y., Huang, H., Qiu, Z., Chen, J., Yang, X., 2012b. Monitoring Change and Position of
540 Coastlines from Satellite Images Using Slope Correction in a Tidal Flat: A Case Study in
541 the Yellow River Delta. Acta Geographica Sinica, 67(3): 377-387.
542 Liu, Y., Huang, H., Qiu, Z., Fan, J., 2013. Detecting coastline change from satellite images based
543 on beach slope estimation in a tidal flat. International Journal of Applied Earth Observation
544 and Geoinformation, 23: 165-176.
545 Mason, D.C., Davenport, I.J., 1996. Accurate and efficient determination of the shoreline in ERS-1
546 SAR images. Geoscience and Remote Sensing, IEEE Transactions on, 34(5): 1243-1253.
547 Miao, C., Shi, W., Chen, X., Yang, L., 2012a. Spatio-temporal variability of streamflow in the
548 Yellow River: possible causes and implications. Hydrological Sciences Journal, 57(7):
549 1355-1367.
550 Miao, C.Y., Ni J.R. Borthwick A.G.L., Yang, L., 2011. A preliminary estimate of human and natural
551 contributions to the changes in water discharge and sediment load in the Yellow River.
552 Global and Planetary Change, 76(3-4): 196-205.
553 Miao, C.Y., Ni J.R., 2009. Variation of Natural Streamflow since 1470 in the Middle Yellow River,
554 China. International Journal of Environmental Research and Public Health, 6(11):
555 2849-2864.
556 Miao, C.Y., Yang L., Chen, X.H., 2012b. The vegetation cover dynamics (1982–2006) in different
557 erosion regions of the Yellow River Basin, China. Land Degradation & Development,

23(1): 62-71.

Miao, C.Y., Ni J.R. Borthwick A.G.L., 2010. Recent changes of water discharge and sediment load in the Yellow River basin, China. Progress in Physical Geography, 34(4):541-561.

Mikhailova, M., 2003. Transformation of the Ebro River Delta under the impact of intense human-induced reduction of sediment runoff. Water Resources, 30(4): 370-378.

Milliman, J.D., Meade, R.H., 1983. World-wide delivery of river sediment to the oceans. The Journal of Geology, 91(81): 1-21.

Ottinger, M., Kuenzer, C., Liu, G., Wang, S., Dech, S., 2013. Monitoring land cover dynamics in the Yellow River Delta from 1995 to 2010 based on Landsat 5 TM. Applied Geography, 44: 53-68.

Peng, J., Chen, S., Dong, P., 2010. Temporal variation of sediment load in the Yellow River basin, China, and its impacts on the lower reaches and the river delta. Catena, 83(2-3): 135-147.

Ryan, T., Sementilli, P., Yuen, P., Hunt, B., 1991. Extraction of shoreline features by neural nets and image processing. Photogrammetric Engineering and Remote Sensing, 57(7): 947-955.

Snedden, G. A., Cable, J. E., Swarzenski, C., Swenson, E. 2007. Sediment discharge into a subsiding Louisiana deltaic estuary through a Mississippi River diversion. *Estuarine Coastal and Shelf Science, 71*(1-2), 181-193

Sun, T., Paola, C., Parker, G., Meakin, P., 2002. Fluvial fan deltas: Linking channel processes with large-scale morphodynamics. Water Resources Research, 38(8): 1151.

Sun Q.H., et al., 2014. Would the 'real' observed dataset stand up? A critical examination of eight observed gridded climate datasets for China. Environmental Research Letters, 9, 015001 doi:10.1088/1748-9326/9/1/015001.

Syvitski, J.P. et al., 2009. Sinking deltas due to human activities. Nature Geoscience, 2(10): 681-686.

Syvitski, J.P., Saito, Y., 2007. Morphodynamics of deltas under the influence of humans. Global and Planetary Change, 57(3): 261-282.

Tucker, C.J., Grant, D.M., Dykstra, J.D., 2004. NASA's global orthorectified Landsat data set. Photogrammetric engineering and remote sensing, 70(3): 313-322.

Wang, H. et al., 2010. Recent changes in sediment delivery by the Huanghe (Yellow River) to the sea: Causes and environmental implications in its estuary. Journal of Hydrology, 391(3-4): 302-313.

589 Wang, H., Yang, Z., Bi, N., Li, H., 2005. Rapid shifts of the river plume pathway off the Huanghe
590 (Yellow) River mouth in response to water-sediment regulation scheme in 2005. Chinese
591 Science Bulletin, 50(24): 2878-2884.
592 Wang, H., Yang, Z., Saito, Y., Liu, J.P., Sun, X., 2006a. Interannual and seasonal variation of the
593 Huanghe (Yellow River) water discharge over the past 50 years: Connections to impacts
594 from ENSO events and dams. Global and Planetary Change, 50(3-4): 212-225.
595 Wang, S., Hassan, M.A., Xie, X., 2006b. Relationship between suspended sediment load, channel
596 geometry and land area increment in the Yellow River Delta. Catena, 65(3): 302-314.
597 Wang, S., Yan, M., Yan, Y., Shi, C., He, L., 2012. Contributions of climate change and human
598 activities to the changes in runoff increment in different sections of the Yellow River.
599 Quaternary International, 282: 66-77.
600 Xu J. X., 2000. Grain-size characteristics of suspended sediment in the Yellow River, China, Catena,
601 38(3): 243-263.
602 Xu, J., 2005. The water fluxes of the Yellow River to the sea in the past 50 years, in response to
603 climate change and human activities. Environmental management, 35(5): 620-631.
604 Xu, X., Guo, H., Chen, X., Lin, H., Du, Q., 2002. A multi-scale study on land use and land cover
605 quality change: the case of the Yellow River Delta in China. GeoJournal, 56(3): 177-183.
606 Yang, S.L., Milliman, J.D., Li, P., Xu, K., 2011. 50,000 dams later: Erosion of the Yangtze River
607 and its delta. Global and Planetary Change, 75(1-2): 14-20.
608 Yang, W., 2012. Shifting of coastline and evolution of tidal flat in modern Yellow River Delta.
609 Marine Geology Frontiers, 28(07): 17-23.
610 Yang, Z., Milliman, J., Galler, J., Liu, J., Sun, X., 1998. Yellow River's water and sediment
611 discharge decreasing steadily. Eos, Transactions American Geophysical Union, 79(48):
612 589-592.
613 Yu, J. et al., 2011. Effects of water discharge and sediment load on evolution of modern Yellow
614 River Delta, China, over the period from 1976 to 2009. Biogeosciences, 8(9): 2427-2435.
615 Yu, L., 2002. The Huanghe (Yellow) River: a review of its development, characteristics, and future
616 management issues. Continental Shelf Research, 22(3): 389-403.
617 Zhang, G., Wang, L., Liu, D., 1998. Biodiversity and Its conservation in the Yellow River Delta
618 Nature Reserve (In Chinese). Rural Eco-Environment, 14: 16-18.
619 Zhang, T. et al., 2011. Assessing impact of land uses on land salinization in the Yellow River Delta,

China using an integrated and spatial statistical model. Land Use Policy, 28(4): 857-866.

Zhang, W., Ruan, X. H., Zheng, J. H., Zhu, Y. L., Wu, H. X. 2010. Long-term change in tidal dynamics and its cause in the Pearl River Delta, China. Geomorphology, 120(3-4), 209-223.

Zhang, X., Wang, L., Si, F., 2001. Prediction of water consumption in the Huanghe river basin. Water Resources and Hydropower Technology, 6: 8-13.

628 Table 1. List of satellite images used in the present work.

Acquisition data	Image type	Resolution (m)	Bands	Acquisition date	Image type	Resolution (m)	Bands
07/07/1983	MSS	80	4	09/08/1998	TM	30	7
07/06/1984	MSS	80	4	06/04/1999	TM	30	7
06/09/1985	TM	30	7	08/04/2000	TM	30	7
08/08/1986	TM	30	7	06/06/2001	ETM+	30	8
08/06/1987	TM	30	7	29/09/2002	ETM+	30	8
10/06/1988	TM	30	7	07/08/2003	TM	30	7
15/07/1989	TM	30	7	05/05/2004	TM	30	7
16/06/1990	TM	30	7	03/07/2005	ETM+	30	8
06/08/1991	TM	30	7	04/06/2006	ETM+	30	8
07/07/1992	TM	30	7	07/06/2007	ETM+	30	8
08/06/1993	TM	30	7	12/08/2008	ETM+	30	8
30/08/1994	TM	30	7	07/08/2009	TM	30	7
18/09/1995	TM	30	7	11/09/2010	TM	30	7
02/07/1996	TM	30	7	02/06/2011	ETM+	30	8
06/08/1997	TM	30	7				

629

630

631 Table 2 Flushings of the Xiaolangdi Reservoir to regulate water discharge and sediment load

Year	Released water discharge (10^9 m^3)	Proportion of water discharge released for total delivery to the sea (%)	Released sediment load (10^6 t)	Proportion of sediment load released for total delivery to the sea (%)
2002	2.32	55.4	50.4	92.8
2003	2.77	14.4	115.1	31.2
2004	4.73	23.8	70.7	27.4
2005	4.18	20.2	45.6	23.9
2006	4.81	25.1	64.8	43.5
2007	6.18	30.3	97.3	66.2
2008	4.18	28.7	64.9	84.2
2009	3.49	26.2	34.5	61.5
2010	9.01	46.7	70.1	41.9
2011	3.73	20.2	41.2	44.5
Total	45.39	26.8	654.6	41.9

632

633

634 Table 3. Error assessment of estimated length of coastline due to daily tidal-induced fluctuations

Year	Error (%)	Year	Error (%)
1983	0.87	1998	0.95
1984	0.92	1999	1.03
1985	0.95	2000	0.99
1986	0.86	2001	0.98
1987	0.88	2002	1.09
1988	0.86	2003	1.05
1989	0.88	2004	1.00
1990	0.97	2005	1.01
1991	0.95	2006	1.05
1992	1.06	2007	1.06
1993	0.92	2008	1.07
1994	1.00	2009	1.06
1995	0.99	2010	1.06
1996	0.91	2011	1.00
1997	1.01	-	-

635

636

637 **Figure Captions**

638 Figure 1. Location of the Yellow River Delta (a) and the study area (b).

639 Figure 2. Runoff (a) and sediment load (b) at Lijin hydrological station from 1983 to 2011.

640 Figure 3. Annual average precipitation and annual average temperature in the Yellow River Basin
641 from 1983 to 2011.

642 Figure 4. No-flow days at Lijin of the Yellow River from 1986 to 2011.

643 Figure 5. Annual runoff (a) and sediment load (b) at the Sanmenxia and Huayuankou hydrological
644 stations from 1983 to 2011.

645 Figure 6. Area changes to the Yellow River Delta from 1983 to 2011.

646 Figure 7. Satellite images showing changes to the Yellow River Delta in different years. The
647 coastline is drawn on the pseudo-color image, with reference to the gray image in the upper
648 right corner.

649 Figure 8. Coastline migration of the Yellow River Delta from 1983 to 2011.

650 Figure 9. Temporal variation of the length of Yellow River Delta coastline from 1983 to 2011.

651 Figure 10. Temporal variation of delta radius ratio for the Yellow River Delta from 1983 to 2011.

652 Figure 11. Satellite images showing the changing morphology of the Yellow River delta lobes at
653 Qingshuigou and Qing 8 in selected years from 1983 to 2011.

654 Figure 12. Relationship between the annual sediment load and annual change of delta area: (a)
655 before and (b) after the artificial diversion from Qingshuigou to Qing 8 in 1996.

656

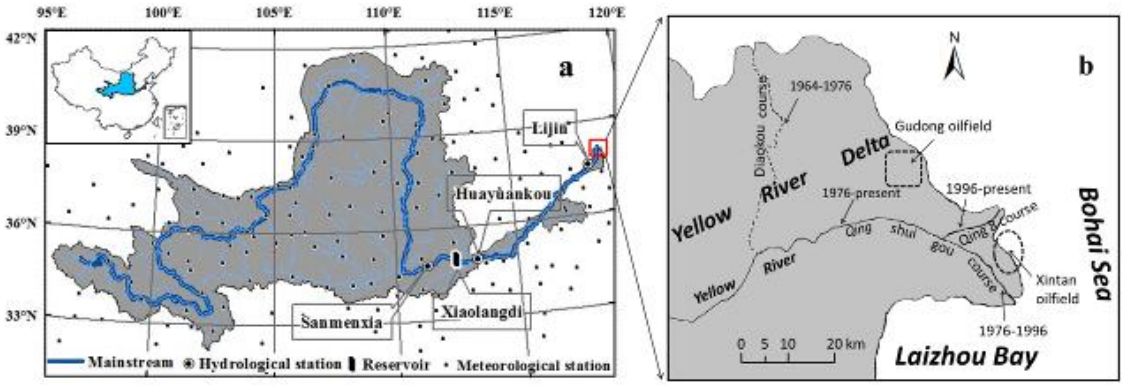

Figure 1. Location of the Yellow River Delta (a) and the study area (b).

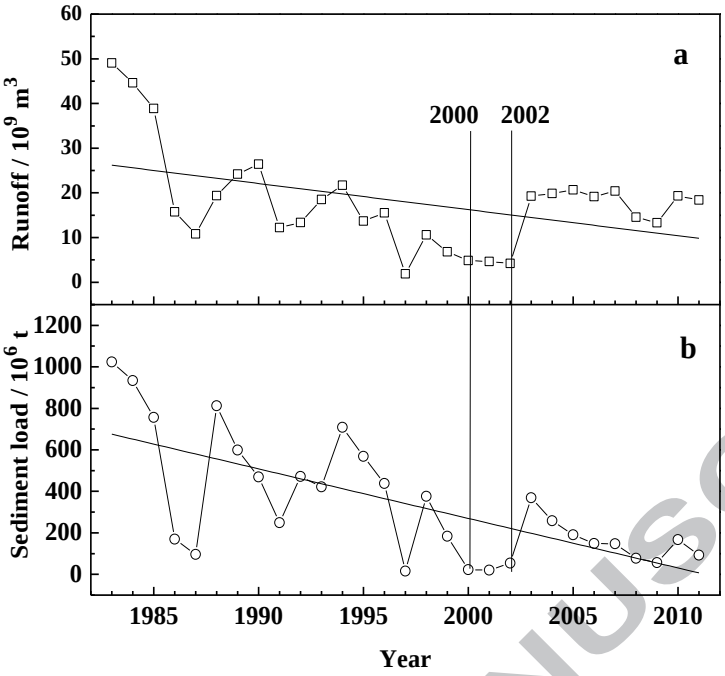

660

661 Figure 2. Runoff (a) and sediment load (b) at Lijin hydrological station from 1983 to 2011.

662

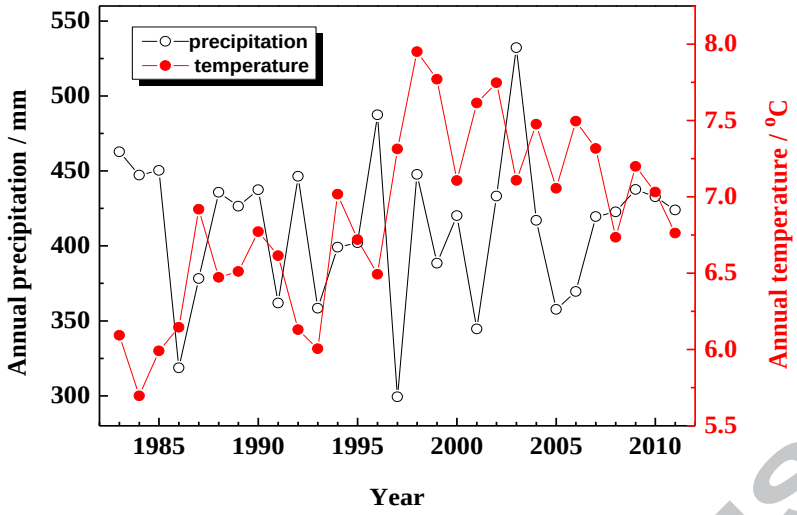

663

664 Figure 3. Annual average precipitation and annual average temperature in the Yellow River Basin

665 from 1983 to 2011.

666

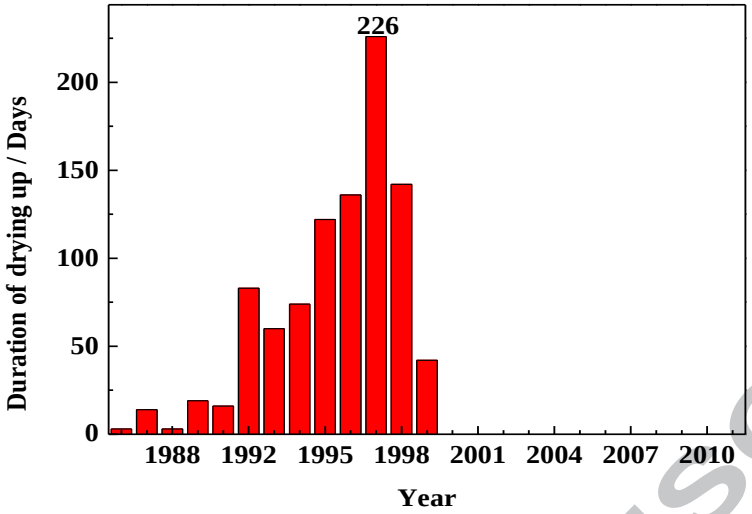

667

668 Figure 4. No-flow days at Lijin of the Yellow River from 1986 to 2011.

669

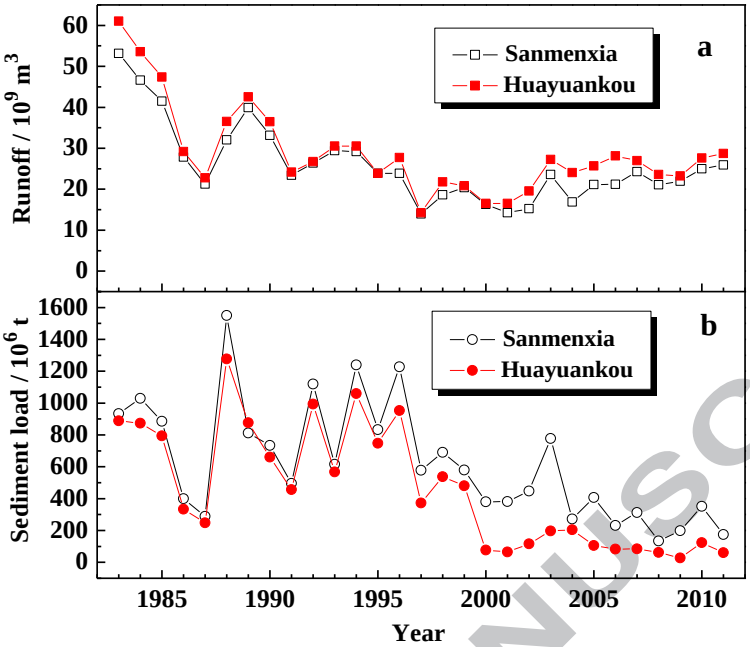

670

671 Figure 5. Annual runoff (a) and sediment load (b) at the Sanmenxia and Huayuankou hydrological

672 stations from 1983 to 2011.

673

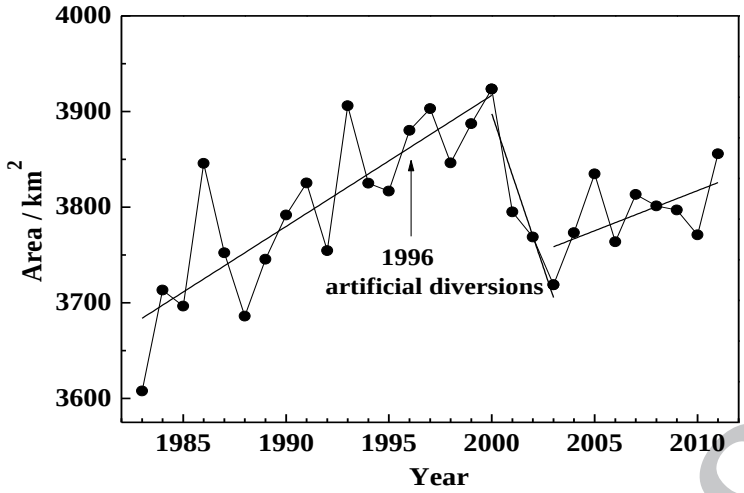

674

675

676 Figure 6. Area changes to the Yellow River Delta from 1983 to 2011.

677

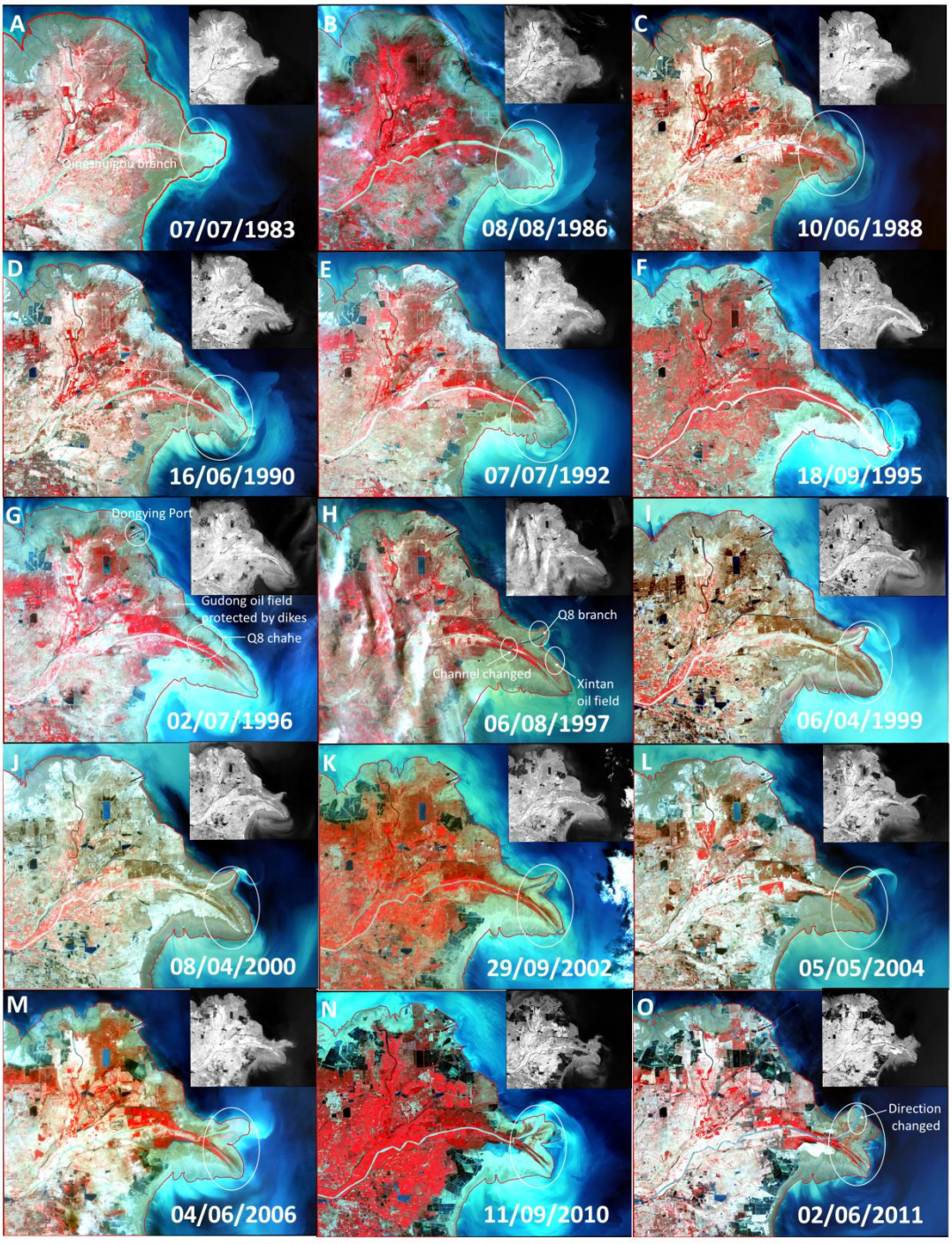

678

679 Figure 7. Satellite images showing changes to the Yellow River Delta in different years. The
680 coastline is drawn on the pseudo-color image, with reference to the gray image in the upper
681 right corner.

682

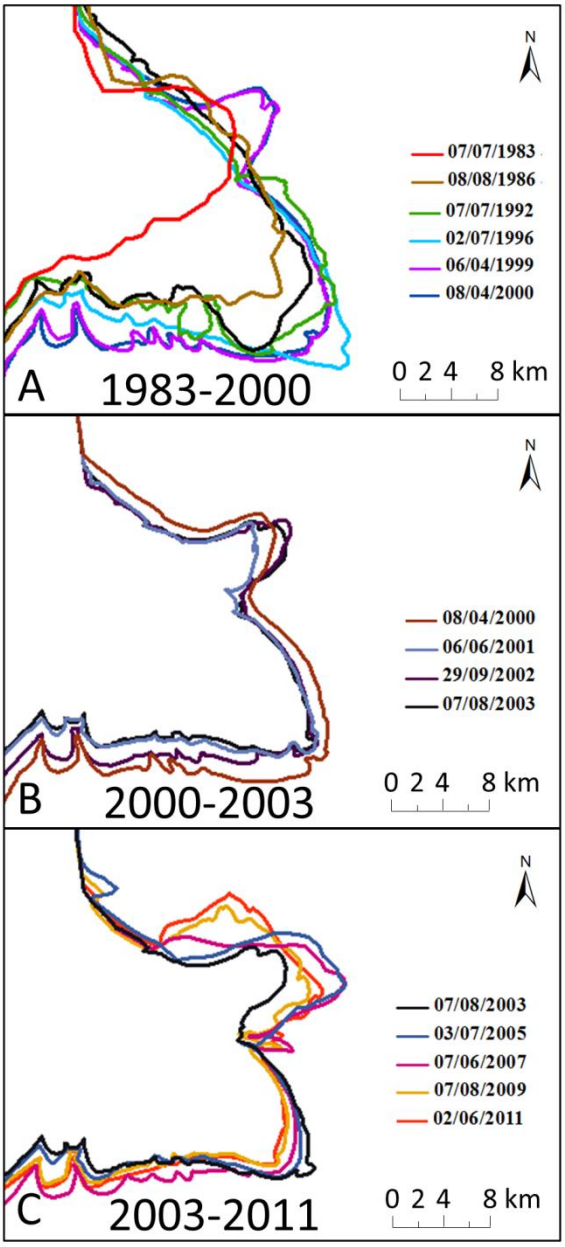

683

684 Figure 8. Coastline migration of the Yellow River Delta from 1983 to 2011

685 .

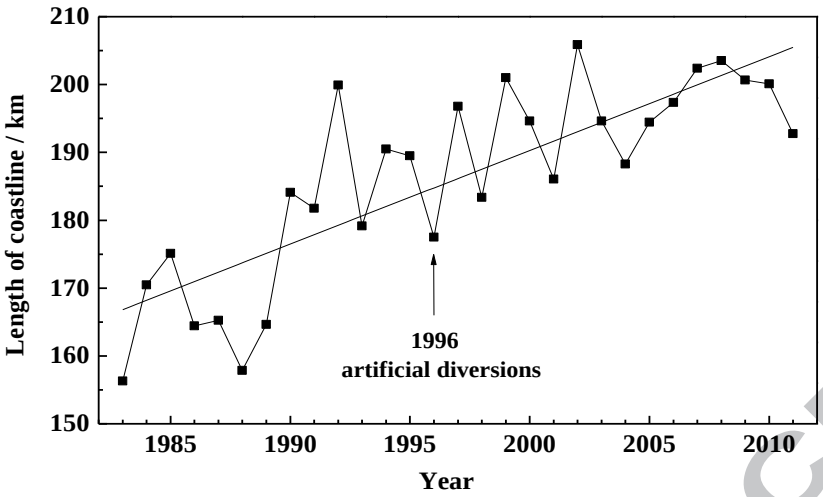

686

687

688 Figure 9. Temporal variation of the length of Yellow River Delta coastline from 1983 to 2011.

689

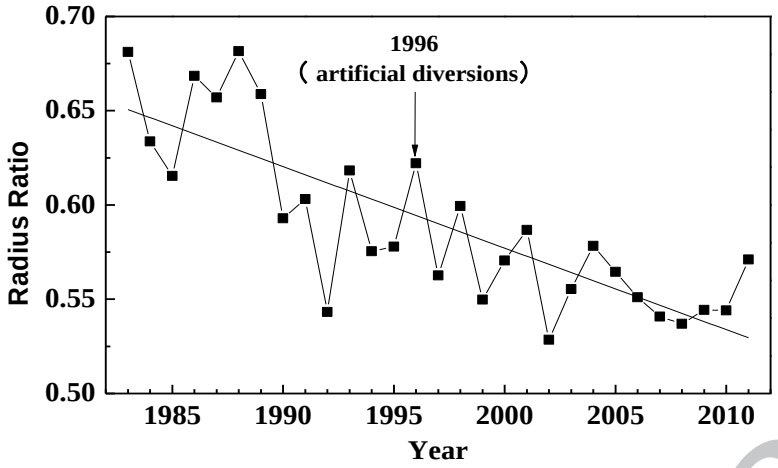

690

691

692 Figure 10. Temporal variation of delta radius ratio for the Yellow River Delta from 1983 to 2011.

693

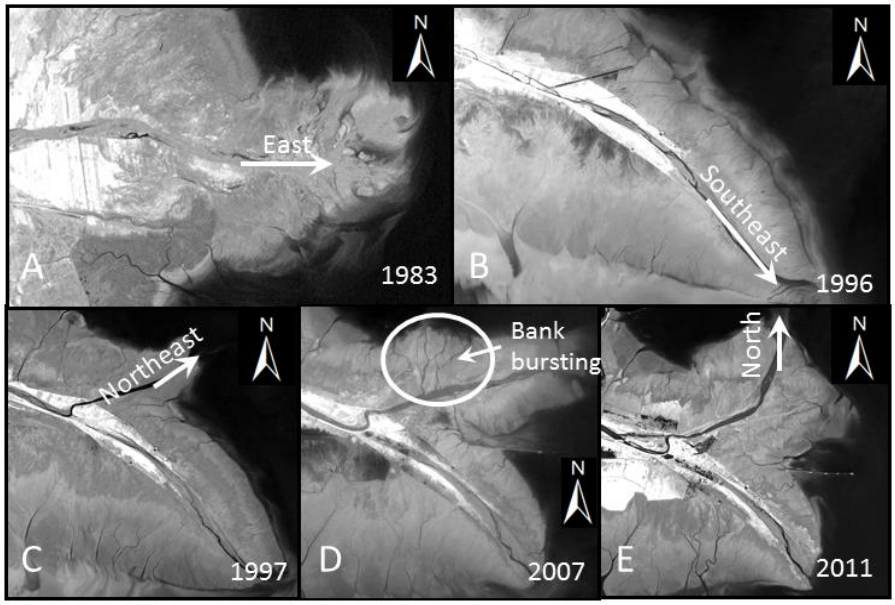

694

695 Figure 11. Satellite images showing the changing morphology of the Yellow River delta lobes at

696 Qingshuigou and Qing 8 in selected years from 1983 to 2011.

697

698

699

700

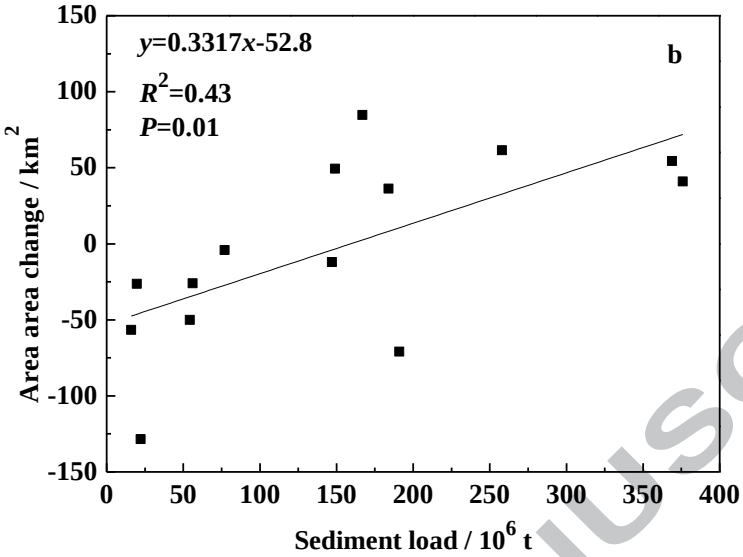

701

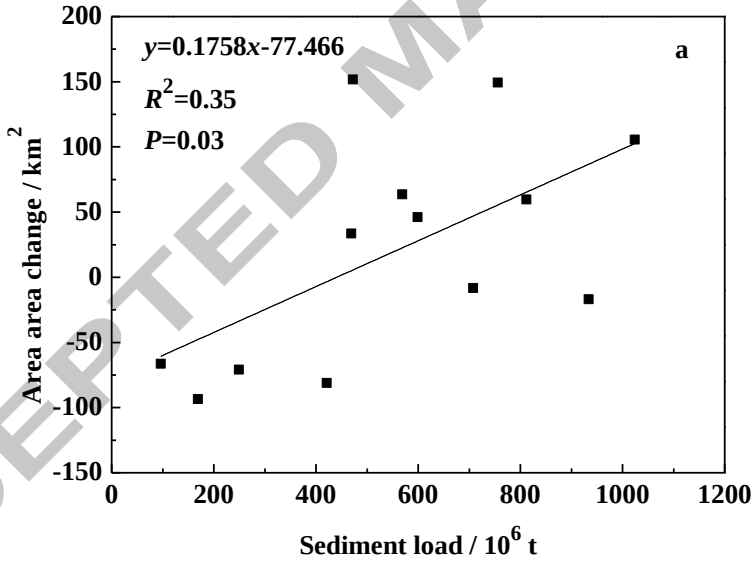

702

703 Figure 12. Relationship between the annual sediment load and annual change of delta area: (a)

704 before and (b) after the artificial diversion from Qingshuigou to Qing 8 in 1996.

705

Highlights

29-year satellite images were used to explore the evoluation of Yellow River Delta;

The morphology of YRD is characterized by a new index defined as delta radius ratio;

The area and coastline of YRD increased by 248 km^2 and 36.45 km, respectively;

YRD required sediment loads of ~ 441×10^6 t yr^{-1} before 1996 to maintain equilibrium;

YRD required sediment loads of ~ 159×10^6 t yr^{-1} after 1996 to maintain equilibrium;